Fractionalized Metal in a Falicov-Kimball Model

Martin Hohenadler and Fakher F. Assaad
Institut für Theoretische Physik und Astrophysik, Universität Würzburg, 97074 Würzburg, Germany

(Received 24 April 2018; published 21 August 2018)

Quantum Monte Carlo simulations reveal an exotic metallic phase with a single-particle gap but gapless spin and charge excitations and a nonsaturating resistivity in a two-dimensional SU(2) Falicov-Kimball model. An exact duality between this model and an unconstrained slave-spin theory leads to a classification of the phase as a fractionalized or orthogonal metal whose low-energy excitations have different quantum numbers than the original electrons. Whereas the fractionalized metal corresponds to the regime of disordered slave spins, the regime of ordered slave spins is a Fermi liquid. At a critical temperature, an Ising phase transition to a spontaneously generated constrained slave-spin theory of the Hubbard model is observed.

DOI: 10.1103/PhysRevLett.121.086601

The fractionalization of electrons into objects with new quantum numbers is among the most fascinating consequences of strong interactions. It is ubiquitous in one-dimensional (1D) metals, where Fermi liquid theory breaks down completely and the low-energy properties are instead determined by collective charge and spin excitations [1]. Fractionalization is less common but physically even richer in higher dimensions, where it involves emergent degrees of freedom such as spinons or gauge fields [2]. A prime example is a genuine Mott insulator without magnetic order that can be classified as a topologically ordered quantum spin liquid [3,4]. Experiments on, e.g., high-temperature superconductors also reveal strange metallic states at higher temperatures such as non-Fermi liquids [5] or bad metals [6], which are believed to be strongly tied to the exotic low-temperature physics. In orthogonal metals [7], with Fermi-liquid-like transport and thermodynamics but no quasiparticles, non-Fermi-liquid physics arises from fractionalization and reconciles the absence of quasiparticles in photoemission with a Fermi surface according to quantum oscillation measurements [7]. Finally, unusual metallic states have become a focus of applications of the gauge-gravity duality [8–10].

Recent insights into fractionalized phases have in particular come from exactly solvable models [7,10–12] and designer Hamiltonians suitable for quantum Monte Carlo (QMC) simulations [13–15]. However, the corresponding models have only limited overlap with the standard models of condensed matter theory. Among the latter, the Hubbard model [16] continues to attract interest [17–19], in significant part due to its expected relevance for high-temperature superconductivity. The Falicov-Kimball model (FKM) [20] is much simpler because electrons of one spin sector remain localized [16]. It admits an exact solution in infinite dimensions where it exhibits a quantum phase transition [21], as well as exact mathematical theorems [22]. FKMs are also instrumental to understand correlated electrons out of equilibrium [23]. While traditionally not associated with the intricate physics of fractionalization, they have recently emerged in the context of lattice gauge theories [24,25]. Finally, FKMs of spinless fermions have been shown to exhibit localization without disorder [26,27].

In this Letter, we show that a fractionalized metallic phase emerges in QMC simulations of a simple 2D FKM. This model has no exact solution, but instead reduces to the Hubbard model at $T = 0$ and/or in infinite dimensions. The observed physics can be understood by exploiting an exact relation to an unconstrained Ising lattice gauge theory via a slave-spin representation. Mean-field arguments reveal the basic mechanism for fractionalization, whereas our simulations fully account for quantum and thermal fluctuations to establish the existence of such a phase in this model.

Model.—We consider the Hamiltonian

$$\hat{H} = -t\sum_{\langle ij\rangle\sigma}(c^{\dagger}_{i\sigma}c_{j\sigma} + \text{H.c.}) - U\sum_{i}\hat{Q}_i\prod_{\sigma}\left(\hat{n}_{i\sigma} - \frac{1}{2}\right). \quad (1)$$

Here, $c^{\dagger}_{i\sigma}$ creates a spin-σ electron at site i of a square lattice and $\hat{n}_{i\sigma} = c^{\dagger}_{i\sigma}c_{i\sigma}$. The first term describes nearest-neighbor hopping. Restricting σ to a single value yields a standard FKM [20] with the localized fermions expressed in terms of the Ising degrees of freedom $\hat{Q}_i = \pm 1$ via the relation $\hat{n}^{\text{loc}}_i = (\hat{Q}_i - 1)/2$. For two flavors $\sigma = \uparrow, \downarrow$, the second term in Eq. (1) becomes a three-body interaction of the Hubbard-Ising form $U\sum_i\hat{Q}_i(\hat{n}_{i\uparrow} - \frac{1}{2})(\hat{n}_{i\downarrow} - \frac{1}{2})$. Generalizations to SU($N$) fermions with $N > 2$ flavors or higher-spin $\hat{Q}_i$ variables are also conceivable. For $N > 1$, the product over flavors renders Eq. (1) not exactly solvable even in infinite dimensions; we consider $N = 2$ in the following. The Ising variables $\hat{Q}_i$ are locally conserved, $[\hat{H}, \hat{Q}_i] = 0$. At the particle-hole symmetric point investigated here, Eq. (1) has an $\text{O}(4) = \text{SO}(4) \times \text{Z}_2$ symmetry. The SO(4) symmetry is the same as for the Hubbard model [28]. The global Z_2 symmetry reflects invariance under $\hat{Q}_i \to -\hat{Q}_i$ in combination with a particle-hole transformation [29] that yields $U \to -U$; it can be broken at $T > 0$ in the 2D case considered.

We use units in which $k_B = t = 1$ and consider periodic $L \times L$ lattices. Simulations were done using the auxiliary-field QMC method [30] from the Algorithms for Lattice Fermions library [31], see also the Supplemental Material [32].

Ising phase transition.—Similar to other FKMs [21], we find a finite-temperature phase transition. In our model, the latter corresponds to a ferromagnetic phase transition of the Ising variables $\hat{Q}_i$ at a critical temperature T_Q that reduces the symmetry from O(4) to SO(4). Its origin can be traced back to an exchange coupling $J\sum_{ij}\hat{Q}_i\hat{Q}_j$—mediated by the itinerant fermions—that is allowed by the symmetries of Eq. (1) and hence generated. The onset of order is visible from the squared magnetization per site $m_Q^2 = M_Q^2/L^2$, where $M_Q^2 = (1/L^2)\sum_{ij}\langle\hat{Q}_i\hat{Q}_j\rangle$, shown in Fig. 1(a). The 2D Ising universality is revealed by the finite-size scaling in Fig. 1(b) with exponents $\beta = 1/8$ and $\nu = 1$. For the phase diagram in Fig. 1(c), we estimated the critical temperature from $m_Q^2(T_Q) = 0.5$ using $L = 8$ and $L = 12$. The dependence of T_Q on U is reminiscent of T_c for the charge-density-wave (CDW) transition of the spinless, half-filled FKM [37,38]. In particular, $T_Q = 0$ at $U = 0$ due to the absence of exchange interactions, and $T_Q \to 0$ for $U \to \infty$ because $T_Q \sim J \sim t^2/U$.

Upon replacing the Ising variables $\hat{Q}_i$ by mean-field values $\langle\hat{Q}_i\rangle = 0$ (for $T > T_Q$) or $\langle\hat{Q}_i\rangle = m_Q$ (for $T < T_Q$), the SU(2) FKM of Eq. (1) reduces to free fermions ($T > T_Q$) or a Hubbard model ($T < T_Q$). We have verified that below T_Q we quantitatively recover Hubbard model results for $T \to 0$ [39], namely, an antiferromagnetic Mott insulator ($m_Q = -1$) or coexisting CDW order and s-wave superconductivity ($m_Q = +1$), respectively [40].

Two distinct metallic regimes.—The novel physics of this Letter occurs at $T > T_Q$, where we find two distinct metallic regimes. A mean-field solution of Eq. (1) with $\langle\hat{Q}_i\rangle = 0$ accounts for the Fermi liquid observed at weak U. The fractionalized metal at large U will naturally emerge from a slave-spin mean-field theory below. The two different metallic regimes indicated in Fig. 1(c) are revealed by the QMC results in Fig. 2. The spin-averaged single-particle spectral function $A(\boldsymbol{k},\omega) = -\pi^{-1}\mathrm{Im}\,G(\boldsymbol{k},\omega)$ calculated from the Green functions $G_\sigma(\boldsymbol{k},\tau) = \langle c^\dagger_{\boldsymbol{k}\sigma}(\tau)c_{\boldsymbol{k}\sigma}(0)\rangle$ via analytic continuation [32] exhibits coherent, gapless excitations in the Fermi-liquid regime at $U = 2$ [Fig. 2(a)].

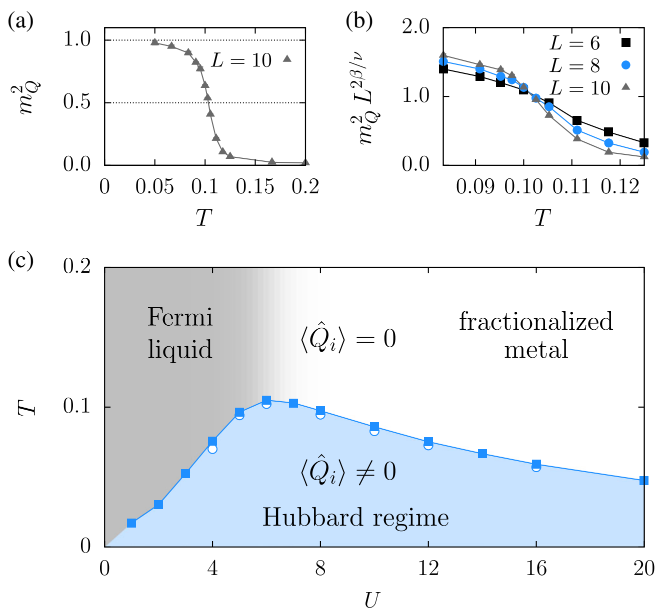

FIG. 1. (a),(b) Ising phase transition for $U = 6$ and (c) phase diagram of the FKM [Eq. (1)] from QMC simulations. The Ising variables $\hat{Q}_i$ order ferromagnetically at a critical temperature T_Q, as revealed by (a) the squared magnetization m_Q^2 and (b) the finite-size scaling with 2D Ising critical exponents. (c) Phase diagram with a high-temperature phase where $\langle\hat{Q}_i\rangle = 0$ and a low temperature phase where $\langle\hat{Q}_i\rangle \neq 0$. The disordered phase at $T > T_Q$ consists of two regimes. The Fermi liquid for $U \lesssim 4$ and the fractionalized metal for $U \gtrsim 4$ are connected by a continuous crossover qualitatively indicated by the color gradient. T_Q was estimated from $m_Q^2(T_Q) = 0.5$ using $L = 8$ (solid symbols) and $L = 12$ (open symbols), respectively.

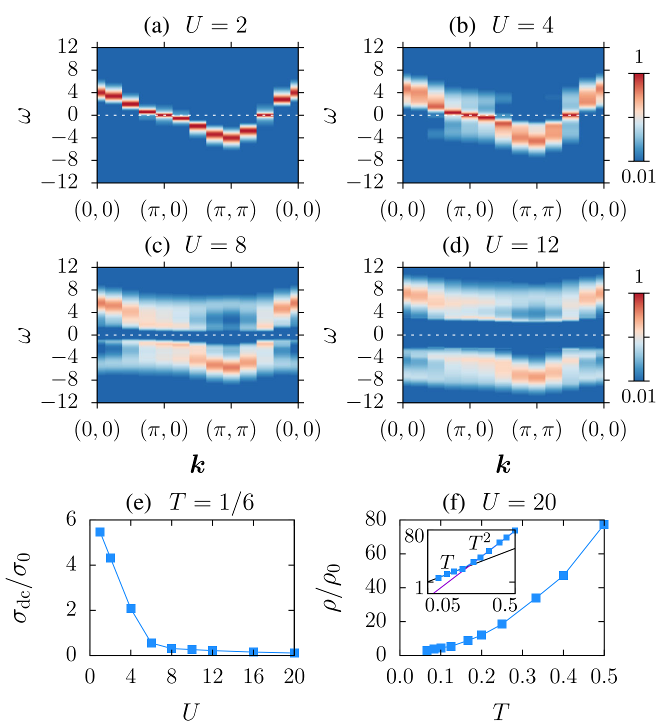

FIG. 2. (a)–(d) Single-particle spectral function $A(\boldsymbol{k},\omega)$ at temperature $T = 1/6$. (e) Conductivity and (f) resistivity $\rho = 1/\sigma_{\mathrm{dc}}$ (inset: logarithmic scales). Here, $L = 8$.

For $U \approx 4$, we observe the opening of a gap that grows with increasing U. At $U = 12$, the spectrum exhibits a large gap and significant broadening [Fig. 2(d)], i.e., no signatures of Landau quasiparticles. According to Fig. 2(e), the conductivity σ_{dc} [32] decreases sharply in the Fermi liquid before saturating at a nonzero value in the fractionalized metal. Finite-size scaling is consistent with $\sigma_{\mathrm{dc}} > 0$ for $L \to \infty$; moreover, in the fractionalized regime, σ_{dc} increases for $T \to 0$ whereas the single-particle spectral weight at $\omega = 0$ decreases strongly [32]. Even for $U = 20$, we find metallic behavior in terms of a resistivity $\rho = 1/\sigma_{\mathrm{dc}}$ that increases without saturation with increasing T [Fig. 2(f); the inset suggests a crossover from $\rho \sim T$ to $\rho \sim T^2$].

Fermi liquid theory cannot reconcile an apparent single-particle gap [32] with metallic behavior. However, these features do co-occur in the pseudogap phase of the attractive Hubbard model at $T_c < T < T^*$ where electrons are bound into uncondensed singlets ($T_c = 0$ for superconductivity at half filling) [41]. In contrast to such a paired Fermi liquid, the fractionalized metal has strongly renormalized but gapless long-wavelength (i.e., $\boldsymbol{q} \to 0$) spin excitations, as visible from the dynamic spin structure factor $S^z(\boldsymbol{q}, \omega)$ [32] in Fig. 3(a). These excitations give rise to a substantial spin susceptibility $\chi_{\mathrm{s}} = \beta(\langle \hat{M}^2 \rangle - \langle \hat{M} \rangle^2)$ (here, $\hat{M} = \sum_i \hat{S}_i^z$) down to $T_Q \sim t/U^2$, see Fig. 3(b); this behavior is again beyond Fermi liquid theory where a single-particle gap implies $\chi_{\mathrm{s}} \to 0$ for $T \to 0$. The results for the attractive Hubbard model in Fig. 3(b) instead exhibit an exponential suppression of χ_{s} below $T^* \sim U$ [42]. Because of the O(4) symmetry at half filling, the spin structure factor and the spin susceptibility of the FKM are identical to their charge counterparts. Hence, Fig. 3 also suggests the existence of gapless charge excitations and hence a metallic state. Finally, the repulsive Hubbard model has a single-particle gap and gapless spin excitations [Fig. 3(b)] but an exponentially suppressed charge susceptibility [identical to χ_{s} of the attractive model in Fig. 3(b)]. In contrast to Fig. 2(f), its resistivity decreases with increasing T, corresponding to insulating behavior [32]. Our data support a fractionalized metal that combines the metallic behavior of the attractive Hubbard model with the gapless spin excitations of the repulsive Hubbard model to yield a non-Fermi-liquid, fermionic metal.

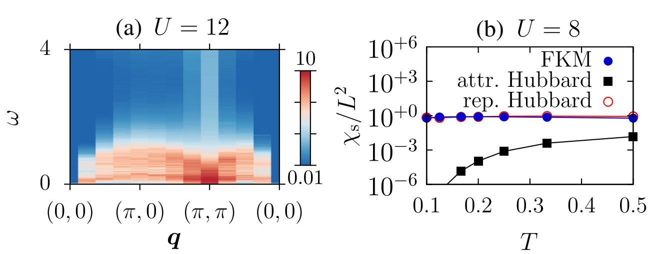

FIG. 3. (a) Dynamic spin structure factor and (b) spin susceptibility of the FKM for $T = 1/6$ and $L = 8$. (b) also shows results for the attractive and the repulsive Hubbard model.

Duality and fractionalization.—To connect the distinct properties observed in the metallic regime at large U to fractionalization, we exploit a duality transformation between the FKM [Eq. (1)] and an unconstrained $\mathbb{Z}_2$ slave-spin theory. To arrive at the latter, we first relabel the states of the local Hilbert space from $\{|0\rangle_i, |\uparrow\rangle_i, |\downarrow\rangle_i, |\uparrow\downarrow\rangle_i\}_c \otimes \{|+1\rangle_i, |-1\rangle_i\}_Q$ to $\{|0\rangle_i, |\uparrow\rangle_i, |\downarrow\rangle_i, |\uparrow\downarrow\rangle_i\}_f \otimes \{|\uparrow\rangle_i, |\downarrow\rangle_i\}_s$. Next, we make the replacements [43]

$$c_{i\sigma}^{(\dagger)} \mapsto f_{i\sigma}^{(\dagger)} \hat{s}_i^z, \qquad \hat{Q}_i \mapsto \hat{s}_i^x (-1)^{\sum_\sigma f_{i\sigma}^\dagger f_{i\sigma}}. \tag{2}$$

Here, $f_{i\sigma}^{(\dagger)}$ is a fermionic operator and $\hat{s}_i^z$, $\hat{s}_i^x$ correspond to Pauli spin matrices. Using the operator identity $(-1)^{\sum_\sigma f_{i\sigma}^\dagger f_{i\sigma}} \equiv (2\hat{n}_{i\uparrow} - 1)(2\hat{n}_{i\downarrow} - 1)$ yields the slave-spin formulation of the FKM (1),

$$\hat{H}^{fs} = -t \sum_{\langle ij \rangle \sigma} (f_{i\sigma}^\dagger f_{j\sigma} \hat{s}_i^z \hat{s}_j^z + \mathrm{H.c.}) - \frac{U}{4} \sum_i \hat{s}_i^x. \tag{3}$$

Equation (3) locally conserves the $\hat{Q}_i$, $[\hat{H}^{fs}, \hat{Q}_i] = 0$, and corresponds to an unconstrained gauge theory in the sense that we do not impose the Gauss law corresponding to $\hat{Q}_i |\psi\rangle = |\psi\rangle$ or simply $\hat{Q}_i = 1$. This unconstrained theory is an exact slave-spin representation of Eq. (1). Enforcing $\hat{Q}_i = 1$ amounts to projecting onto the 4D local Hilbert space of the Hubbard model and promotes Eq. (3) to an exact (constrained) $\mathbb{Z}_2$ slave-spin theory of the latter. This also becomes apparent from Eq. (1) upon setting $\hat{Q}_i = 1$. An intriguing question is, under what conditions are the constrained and unconstrained theories are equivalent? According to Fig. 1, the constraints $\hat{Q}_i$ are spontaneously generated in the ferromagnetic phase at $T < T_Q$ so that for $T \to 0$ the unconstrained theory [Eq. (3)] becomes an exact slave-spin representation of the Hubbard model. Moreover, the constraints are completely irrelevant at $U = 0$ [where both Eqs. (1) and (3) reduce to free fermions] and in infinite dimensions for any U and T; the latter statement holds only at the particle-hole symmetric point and was previously proved in the slave-spin representation [44]. It also follows directly for the half-filled FKM because the only nonzero contributions in a diagrammatic expansion in the interaction $U \sum_i \hat{Q}_i (\hat{n}_{i\uparrow} - \frac{1}{2})(\hat{n}_{i\downarrow} - \frac{1}{2})$ contain even numbers of vertices at a single site (the free propagator is local for $D = \infty$ [45,46]) and $(\hat{Q}_i)^{2n} = 1$.

A mean-field theory of the dual slave-spin model Eq. (3) captures the metallic state observed at strong coupling and relates it to fractionalization. The product ansatz $|\Phi\rangle_{\mathrm{MF}} = |\phi\rangle_f \otimes |\phi\rangle_s$ for the ground-state decouples the problem into a free-fermion part $\hat{H}_{\mathrm{MF}}^f = -t \sum_{\langle ij \rangle \sigma} g_{ij} (f_{i\sigma}^\dagger f_{j\sigma} + f_{j\sigma}^\dagger f_{i\sigma})$ and a transverse-field Ising model $\hat{H}_{\mathrm{MF}}^s = -t \sum_{\langle ij \rangle} J_{ij} \hat{s}_i^z \hat{s}_j^z - (U/4) \sum_i \hat{s}_i^x$ connected by the self-consistency conditions $g_{ij} = \langle \hat{s}_i^z \hat{s}_j^z \rangle_s$ and $J_{ij} = \sum_\sigma \langle f_{i\sigma}^\dagger f_{j\sigma} + \mathrm{H.c.} \rangle_f$ [43]. The slave spins will be ferromagnetically ordered for $U < U_c$, and disordered for $U > U_c$. The effect of this transition on the original electrons becomes clear from their spectral function, $A(\boldsymbol{k}, \omega) = \langle \hat{s}_i^z \rangle^2 \delta(\omega - E_{\boldsymbol{k}})$ [7], where $E_{\boldsymbol{k}}$ is the f-fermion dispersion. Clearly, $\langle \hat{s}_i^z \rangle^2$ is directly related to the quasiparticle residue Z, which is finite for $U < U_c$ but vanishes for $U > U_c$. Within single-site mean-field theories, including dynamical mean-field theory, this transition is associated with a Mott metal-insulator transition for which $\langle \hat{s}_i^z \rangle$ serves as an order parameter [43,47]. Beyond single-site mean-field theories, $\langle \hat{s}_i^z \hat{s}_j^z \rangle \neq \langle \hat{s}_i^z \rangle^2$, and the disordered phase is an orthogonal metal with Drude weight $D \sim \langle \hat{s}_i^z \hat{s}_j^z \rangle$ rather than a Mott insulator [7].

In the context of slave-spin representations, fractionalization amounts to the dissociation of the physical c electrons into auxiliary f fermions, which carry the physical U(1) charge [7], and the slave spins $\hat{s}_i^z$. Whereas the c fermions are invariant under local gauge transformations generated by the $\hat{Q}_i$, the f fermions and slave spins each carry a Z_2 gauge charge that manifests itself as $\hat{Q}_i f_{i\sigma}^{(\dagger)} \hat{Q}_i = -f_{i\sigma}^{(\dagger)}$, $\hat{Q}_i \hat{s}_i^z \hat{Q}_i = -\hat{s}_i^z$. While this charge is strictly conserved only in constrained gauge theories, the notion of fractionalization remains meaningful in a broader context, including mean-field theories, where the constraints are either ignored or imposed on average [43], and unconstrained gauge theories such as Eq. (3), where the charge is conserved in space but not in time. In particular, the orthogonal metal emerging in mean-field theory at $U > U_c$ from the disordering of the slave spins may be regarded as fractionalized in the sense that the metallic properties are carried by the Z_2-charged f fermions that are orthogonal [7] to the gauge-invariant c fermions.

The mean-field fractionalization scenario is essentially borne out by our QMC results for the FKM: as shown in Fig. 2, the single-particle spectrum has a gap at large U but the system remains metallic. Within our unbiased QMC approach, the mean-field phase transition of the slave spins is replaced by an order-disorder crossover reflected in the slave-spin correlator $G^s(\tau) = \langle \hat{s}_i^z(\tau) \hat{s}_i^z \rangle$ in Fig. 4(a) and directly related to the opening of the single-particle gap in Fig. 2. The disorder of the slave spins strongly enhances scattering and suppresses coherent quasiparticle motion [Fig. 2(e)]. However, the current correlator

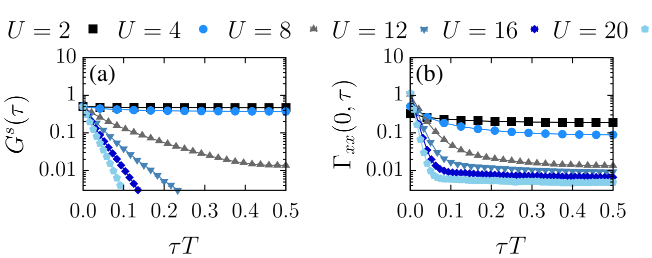

FIG. 4. (a) Slave-spin Green function $G^s(\tau)$ and (b) current-current correlator $\Gamma_{xx}(\boldsymbol{q} = 0, \tau)$ for $L = 8$ and $T = 1/6$.

$\Gamma_{xx}(\boldsymbol{q} = 0, \tau)$ [32] in Fig. 4(b) remains gapless even for large U.

Discussion.—While the non-Fermi-liquid regime at large U exists independent of the slave-spin representation, the latter reveals the fractionalization and close conceptual relations to orthogonal metals [7]. On the other hand, our findings differ in a number of important details from previous mean-field and exact realizations of such states [7]. First, our simulations preserve the local Z_2 gauge symmetry of Eq. (3), in accordance with Elitzur's theorem [48]. This symmetry—reflecting invariance under the local transformation $f_{i\sigma}^{(\dagger)} \mapsto -f_{i\sigma}^{(\dagger)}$, $\hat{s}_i^z \mapsto -\hat{s}_i^z$ generated by $\hat{Q}_i$—implies that the spatial correlations $\langle \hat{s}_i^z \hat{s}_{j\neq i}^z \rangle$ responsible for a nonzero Drude weight in mean-field theory are zero [13]. Accordingly, the slave spins undergo a crossover [in imaginary time, see Fig. 4(a)], instead of a phase transition. Similarly, the f fermions are localized because they also carry Z_2 charge and the gapped but dispersive single-particle excitations in Fig. 2(d) instead emerge from the combination of imaginary-time correlations (i.e., quantum fluctuations) and vertex corrections. If the latter are absent, as in infinite dimensions, a single-particle gap always implies insulating behavior [45]. In this limit, non-Fermi-liquid behavior can arise without fractionalization from spin freezing [49]. Whereas the orthogonal metals in the exactly solvable models of Ref. [7] are noninteracting, transport and thermodynamic properties are strongly renormalized by interactions in the present, correlated fractional metal. Finally, in contrast to the t-J model with random interaction [10], our fractionalized phase arises in a fully translation-invariant setting.

Our work has connections to several other areas of current interest. A 1D unconstrained gauge theory (equivalent to a spinless FKM) was recently shown to exhibit localization without disorder [27]. The quantum percolation mechanism in the 2D case [25] may be connected to the metallic behavior observed here. At high temperatures, our Falicov-Kimball problem becomes equivalent to a Hubbard model with an annealed, disordered interaction $U_i = \pm U$. For bosons, a random Hubbard interaction supports many-body localization [50]. The slave-spin formulation [Eq. (3)] provides a link to recent simulations of lattice gauge theories coupled to fermions that exhibit exotic phases and phase transitions [13–15], as well as to Sachdev-Ye-Kitaev models [10]. Progress on cold-atom realizations of FKMs and Hubbard models [19,51,52] as well as lattice gauge theories [53] even promises the possibility of experimentally observing the fractionalized metal, facilitated by its stability at high temperatures.

In summary, we have presented unbiased numerical evidence for a non-Fermi-liquid phase in a simple 2D Falicov-Kimball model. This Fermi metal differs from phases of incoherently paired fermions (i.e., bosons) such as the paired Fermi liquid known from the attractive Hubbard model, and previous realizations of orthogonal metals. The exact relation to an unconstrained slave-spin representation allowed us to understand the physics in terms of fractionalization of the original electrons.

We thank M. Fabrizio and A. Honecker for helpful discussions. This work was supported by the DFG through SFB 1170 ToCoTronics. We thank the John von Neumann Institute for Computing (NIC) for computer resources on the JURECA [54] machine at the Jülich Supercomputing Centre (JSC).

[1] T. Giamarchi, *Quantum Physics in One Dimension* (Clarendon Press, Oxford, 2004).
[2] E. Fradkin, *Field Theories of Condensed Matter Physics* (Cambridge University Press, Cambridge, England, 2013).
[3] M. B. Hastings, Phys. Rev. B **69**, 104431 (2004).
[4] Y. Zhou, K. Kanoda, and T.-K. Ng, Rev. Mod. Phys. **89**, 025003 (2017).
[5] A. J. Schofield, Contemp. Phys. **40**, 95 (1999).
[6] V. J. Emery and S. A. Kivelson, Phys. Rev. Lett. **74**, 3253 (1995).
[7] R. Nandkishore, M. A. Metlitski, and T. Senthil, Phys. Rev. B **86**, 045128 (2012).
[8] T. Faulkner, N. Iqbal, H. Liu, J. McGreevy, and D. Vegh, Science **329**, 1043 (2010).
[9] S. Sachdev, Phys. Rev. Lett. **105**, 151602 (2010).
[10] W. Fu, Y. Gu, S. Sachdev, and G. Tarnopolsky, arXiv:1804.04130.
[11] A. Kitaev, Ann. Phys. (Amsterdam) **321**, 2 (2006).
[12] Y. Zhong, K. Liu, Y.-Q. Wang, and H.-G. Luo, Phys. Rev. B **86**, 165134 (2012).
[13] F. F. Assaad and T. Grover, Phys. Rev. X **6**, 041049 (2016).
[14] S. Gazit, M. Randeria, and A. Vishwanath, Nat. Phys. **13**, 484 (2017).
[15] S. Gazit, F. F. Assaad, S. Sachdev, A. Vishwanath, and C. Wang, Proc. Natl. Acad. Sci. U.S.A. **115**, E6987 (2018).
[16] J. Hubbard, Proc. R. Soc. A **276**, 238 (1963).
[17] B.-X. Zheng, C.-M. Chung, P. Corboz, G. Ehlers, M.-P. Qin, R. M. Noack, H. Shi, S. R. White, S. Zhang, and G. K. -L. Chan, Science **358**, 1155 (2017).
[18] E. W. Huang, C. B. Mendl, S. Liu, S. Johnston, H.-C. Jiang, B. Moritz, and T. P. Devereaux, Science **358**, 1161 (2017).
[19] A. Mazurenko, C. S. Chiu, G. Ji, M. F. Parsons, M. Kanász-Nagy, R. Schmidt, F. Grusdt, E. Demler, D. Greif, and M. Greiner, Nature (London) **545**, 462 (2017).
[20] L. Falicov and J. Kimball, Phys. Rev. Lett. **22**, 997 (1969).
[21] J. K. Freericks and V. Zlatić, Rev. Mod. Phys. **75**, 1333 (2003).
[22] C. Gruber and N. Macris, Helv. Phys. Acta **69**, 850 (1996).
[23] H. Aoki, N. Tsuji, M. Eckstein, M. Kollar, T. Oka, and P. Werner, Rev. Mod. Phys. **86**, 779 (2014).
[24] C. Prosko, S.-P. Lee, and J. Maciejko, Phys. Rev. B **96**, 205104 (2017).
[25] A. Smith, J. Knolle, R. Moessner, and D. L. Kovrizhin, Phys. Rev. B **97**, 245137 (2018).
[26] A. E. Antipov, Y. Javanmard, P. Ribeiro, and S. Kirchner, Phys. Rev. Lett. **117**, 146601 (2016).
[27] A. Smith, J. Knolle, D. L. Kovrizhin, and R. Moessner, Phys. Rev. Lett. **118**, 266601 (2017).
[28] C. N. Yang and S. Zhang, Mod. Phys. Lett. B **4**, 759 (1990).
[29] H. Shiba, Prog. Theor. Phys. **48**, 2171 (1972).
[30] R. Blankenbecler, D. J. Scalapino, and R. L. Sugar, Phys. Rev. D **24**, 2278 (1981).
[31] M. Bercx, F. Goth, J. S. Hofmann, and F. F. Assaad, SciPost Phys. **3**, 013 (2017).
[32] See Supplemental Material at http://link.aps.org/supplemental/10.1103/PhysRevLett.121.086601 for details about the implementation and measurements, as well as additional data, and which contains Refs. [33–36]
[33] F. F. Assaad and H. G. Evertz, in *Computational Many Particle Physics*, Lecture Notes in Physics, edited by H. Fehske, R. Schneider, and A. Weiße (Springer Verlag, Berlin, 2008), Vol. 739, p. 277.
[34] K. S. D. Beach, arXiv:cond-mat/0403055.
[35] R. T. Scalettar, N. Trivedi, and C. Huscroft, Phys. Rev. B **59**, 4364 (1999).
[36] D. J. Scalapino, S. R. White, and S. Zhang, Phys. Rev. B **47**, 7995 (1993).
[37] M. M. Maśka and K. Czajka, Phys. Rev. B **74**, 035109 (2006).
[38] L. Chen, J. K. Freericks, and B. A. Jones, Phys. Rev. B **68**, 153102 (2003).
[39] M. Hohenadler and F. F. Assaad (to be published).
[40] R. T. Scalettar, E. Y. Loh, J. E. Gubernatis, A. Moreo, S. R. White, D. J. Scalapino, R. L. Sugar, and E. Dagotto, Phys. Rev. Lett. **62**, 1407 (1989).
[41] M. Randeria, N. Trivedi, A. Moreo, and R. T. Scalettar, Phys. Rev. Lett. **69**, 2001 (1992).
[42] R. R. dos Santos, Phys. Rev. B **50**, 635 (1994).
[43] A. Rüegg, S. D. Huber, and M. Sigrist, Phys. Rev. B **81**, 155118 (2010).
[44] M. Schiró and M. Fabrizio, Phys. Rev. B **83**, 165105 (2011).
[45] A. Khurana, Phys. Rev. Lett. **64**, 1990 (1990).
[46] E. Müller-Hartmann, Z. Phys. B **74**, 507 (1989).
[47] R. Žitko and M. Fabrizio, Phys. Rev. B **91**, 245130 (2015).
[48] J. B. Kogut, Rev. Mod. Phys. **51**, 659 (1979).
[49] P. Werner, E. Gull, M. Troyer, and A. J. Millis, Phys. Rev. Lett. **101**, 166405 (2008).
[50] P. Sierant, D. Delande, and J. Zakrzewski, Phys. Rev. A **95**, 021601 (2017).
[51] M. Lewenstein, A. Sanpera, V. Ahufinger, B. Damski, A. Sen, and U. Sen, Adv. Phys. **56**, 243 (2007).
[52] T. Esslinger, Annu. Rev. Condens. Matter Phys. **1**, 129 (2010).
[53] E. Zohar, J. I. Cirac, and B. Reznik, Rep. Prog. Phys. **79**, 014401 (2016).
[54] Jülich Supercomputing Centre, J. Large-Scale Res. Facilities **2**, A62 (2016).